Time-domain response of a metal detector to a target buried in soil with frequency-dependent magnetic susceptibility

Y. Das

Defence R&D Canada – Suffield

P.O. Box 4000, Station Main, Medicine Hat AB, Canada T1A 8K6

ABSTRACT

The work reported in this paper is a part of on-going studies to clarify how and to what extent soil electromagnetic properties affect the performance of induction metal detectors widely used in humanitarian demining. This paper studies the specific case of the time-domain response of a small metallic sphere buried in a non-conducting soil half-space with frequency-dependent complex magnetic susceptibility. The sphere is chosen as a simple prototype for the small metal parts in low-metal landmines, while soil with dispersive magnetic susceptibility is a good model for some soils that are known to adversely affect the performance of metal detectors. The included analysis and computations extend previous work which has been done mostly in the frequency domain. Approximate theoretical expressions for weakly magnetic soils are found to fit the experimental data very well, which allowed the estimation of soil model parameters, albeit in an ad hoc manner. Soil signal is found to exceed target signal (due to an aluminum sphere of radius 0.0127 m) in many cases, even for the weakly magnetic Cambodian laterite used in the experiments. How deep a buried target is detected depends on many other factors in addition to the relative strength of soil and target signals. A general statement cannot thus be made regarding detectability of a target in soil based on the presented results. However, computational results complemented with experimental data extend the understanding of the effect that soil has on metal detectors.

Keywords: landmine detection, humanitarian demining, electromagnetic properties of soil, magnetic susceptibility of soils, magnetic viscosity, pulsed induction metal detectors

1. INTRODUCTION

The electromagnetic induction metal detector is one of the most commonly used tools to detect buried landmines in humanitarian demining. One of the important factors that can influence the signal produced in such a detector is the host soil. A systematic analytical framework, based on well-established techniques in geophysics and non-destructive testing, for studying the effects of soil electromagnetic properties was presented in an earlier paper [1], including a discussion of the relevance and requirements of soil-related research in humanitarian demining. Results of further study and additional numerical results were included in a subsequent paper [2]. Most of the discussion in these previous papers has been based on frequency domain analysis. Since a large number of detectors used in practice employ pulsed transmitter currents, studies in the time domain are considered essential. To that end, the present paper, which is a part of on-going studies to clarify how and to what extent soil electromagnetic properties affect the performance of metal detectors, analyzes the specific case of the time-domain response of a small metallic sphere buried in a soil with frequency-dependent complex magnetic susceptibility. The sphere is chosen as a simple prototype for the small metal parts in low-metal landmines, while soil with dispersive magnetic susceptibility is a good model for some soils [3] that are known to adversely affect the performance of metal detectors.

The analytical results and framework for computation are summarized in Section 2, which also includes a discussion of the specific model for soil magnetic susceptibility used in this paper. A brief description of

experimental set up used to measure the induction response of soil and targets is given in Section 3. Numerical and experimental results for soil and target response are discussed in Section 4. A summary and overall conclusions are given in Section 5.

2. ANALYSIS

The geometry employed to analyze the metal detector problem is the same as the one used in [1, 2] and is repeated in Figure 1. The soil is modelled as a homogeneous halfspace and the metal detector head is taken to consist of a pair of concentric and coplanar circular coils. The transmitter coil radius and number of turns are respectively a and N_t while those of the receiver coil are b and N_r. The coordinate systems used, the magnetic permeability (μ_j), electrical conductivity (σ_j) and permittivity ϵ_j of the various regions are shown on the figure, where the subscript $j = 0, 1, 2$ indicates air, soil and target material respectively. The coil assembly is at a height $z = h$ from the air-soil interface. In the frequency domain, the transmitter current is defined to be $Ie^{i\omega t}$ with $\omega = 2\pi f$, where f is the frequency of operation. Time domain results will be computed from known frequency-domain ones through inverse transforms. Except for some simple cases, where analytical results are available, inversions will be carried out using a numerical technique presented in [4].
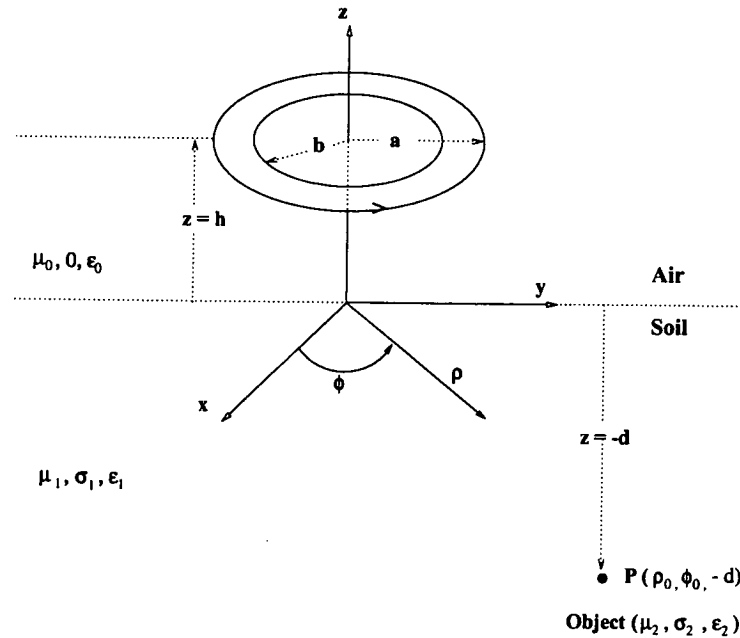

Figure 1. Geometry of the problem.

2.1. Soil Model

In this paper, only the specific case of non-conducting soil ($\sigma_1 = 0$ S/m) with frequency-dependent magnetic susceptibility $\chi(\omega)$ will be considered. As well, the permittivity of soil will be assumed to be frequency-independent, the same as that of free space and will be not be considered in the results (i.e., displacement currents will be ignored). The particular model of magnetic behaviour used in the analysis is as follows:

$$\mu_1 = \mu_0(1 + \chi(\omega)) \tag{1}$$

$$\chi(\omega) = \chi'(\omega) + i\chi''(\omega) = \chi_0 \left(1 - \frac{1}{\ln(\tau_2/\tau_1)} \cdot \ln \frac{i\omega\tau_2 + 1}{i\omega\tau_1 + 1}\right) \tag{2}$$

where μ_0 and μ_1 are the magnetic permeability of free-space and soil respectively. $\chi(\omega)$ is the complex frequency-dependent susceptibility of soil with real and imaginary components χ' and χ'' respectively, while χ_0 is the d.c. value of susceptibility. τ_1 and τ_2 are the lower and upper limits respectively of magnetic relaxation time constants of the soil. This model, which has been discussed in previous work [1, 2, 5–9], is often used to represent soils that display magnetic viscosity. Such soils are common in many landmine-affected regions of the world.

Measurements allowing unique determination of all three parameters of the model, namely, χ_0, τ_1 and τ_2 are not readily available. (Nevertheless, an ad hoc trial-and-error technique of estimating χ_0, τ_1 and τ_2 from available frequency and time-domain data is discussed in Section 4.1). However, an approximation derived from Equation 2 can often be used in conjunction with measurements made by commercial-off-the-shelf equipment to obtain results that are useful in practice. If measurement times and parameter values are such that $\omega\tau_1 \ll 1$ and $\omega\tau_2 \gg 1$ (or equivalently $t/\tau_1 \gg 1$ and $t/\tau_2 \ll 1$), it can be shown from Equation 2 that

$$\frac{\partial \chi'}{\partial \, ln\omega} = \frac{2}{\pi}\chi'' = -\frac{\chi_0}{ln(\tau_2/\tau_1)} \qquad (3)$$

According to this relationship which has been discussed in detail by others [8, 10, 11], the slope (with respect to $ln\omega$) of the real part of susceptibility is constant and is proportional to its imaginary part. In practice, measurements of χ' at two frequencies provided by an instrument such as the popular Bartington MS2B dual-frequency susceptibility meter [12], which measures χ' at 465Hz and at 4650Hz, are used to estimate the required slope assuming linear variation with respect to $ln\omega$. This approximation will be used in parts of this paper to calculate time-domain response of soil. It should be noted that measurements of complex susceptibility over a much wider frequency band [11, 13], albeit for a limited number of soil samples, indicate that the linear approximation may be adequate for some real-world soils.

2.2. Response of Soil

Using results from [1, 2] one can write down the expressions for induced voltages under various conditions. The voltage, normalized by the product N_tN_rI, induced in the receiver coil by a non-conducting ($\sigma_1 = 0$) but magnetic halfspace is given by

$$v^{soil}(\omega) = i\mu_0\omega\pi ab\left[\frac{\chi(\omega)}{2 + \chi(\omega)}\right]m(h) \qquad (4)$$

where $m(h) = \int_0^\infty J_1(\lambda a)J_1(\lambda b)\exp(-2\lambda h)d\lambda$, J_1 denotes a Bessel function of the first kind and order 1, and λ is an integration variable. Using integral no.17 on page 316 in section 13.4.1 of [14] $m(h)$ can be shown to be

$$m(h) = \frac{2}{\pi k\sqrt{ab}}\left[(1 - \frac{1}{2}k^2)K - E\right] \qquad (5)$$

where $k^2 = \frac{4ab}{(a+b)^2+4h^2}$, and K and E are complete elliptic integrals of the first and second kind respectively, defined as $K = \int_0^{\pi/2}\left(1 - k^2sin^2\theta\right)^{-1/2}d\theta$ and $E = \int_0^{\pi/2}\left(1 - k^2sin^2\theta\right)^{1/2}d\theta$.

The frequency-domain expression, Equation 4, can be used to derive time-domain relations through the use of Laplace and Fourier transform theory. For example, the response to a step-current excitation can be derived by calculating the inverse Fourier transform of $v^{soil}(\omega)/(i\omega)$ or, equivalently, by calculating the inverse Laplace transform of $v^{soil}(s)/s$ where the transform variable is defined* by $s = i\omega$. A numerical implementation of this approach using limited frequency-domain data is given in [4]. The author is not aware of any analytical expression for the required inverse transforms when no approximation is made regarding $\chi(\omega)$ in Equation 4, and in such cases use will be made of the numerical technique [4] already noted. However, if the soil is very weakly magnetic ($|\chi| \ll 1$) which is commonly the case with natural soils, the response for $t > 0$ to a step-current excitation that at $t = 0$ can be written as [1]

$$v^{soil}_{step}(t) = \mu_0\pi abm(h)\frac{\chi_0}{2\ln(\tau_2/\tau_1)}\cdot\frac{1}{t} \qquad (6)$$

*Strictly speaking $v^{soil}(\omega)$ and $\chi(\omega)$ should be written as $v^{soil}(i\omega)$ and $\chi(i\omega)$ respectively.

when measurement times and parameter values are such that $\frac{t}{\tau_1} \gg 1$ and $\frac{t}{\tau_2} \ll 1$. The discussion in the literature often centers around the step response. However, the response due to finite current pulses which are used in practice must be considered in the analysis of metal detectors. One common current waveform, which is also the shape used in the experiments for this work, is a short triangular pulse of duration T. Starting from the above step response (Equation 6) and applying Laplace transform theory[†], one can show that the response to a triangular current pulse of duration T and peak value I_0 is given by

$$v^{soil}_{ramp}(t) = \mu_0 \pi abm(h) \frac{\chi_0}{2\ln(\tau_2/\tau_1)} \cdot \frac{I_0}{T} \left(ln\frac{T+t}{t} - \frac{T}{t} \right) \tag{7}$$

where t is measured from current turn-off.

Further simplifications can be obtained by using Equation 3 in Equations 6 and 7:

$$v^{soil}_{step}(t) = -\mu_0 \pi abm(h) \frac{\chi''}{\pi} \cdot \frac{1}{t}$$
$$= -\frac{1}{2}\mu_0 \pi abm(h) \cdot \frac{\partial \chi'}{\partial \, ln\omega} \cdot \frac{1}{t} \tag{8}$$

$$v^{soil}_{ramp}(t) = -\mu_0 \pi abm(h) \frac{\chi''}{\pi} \cdot \frac{I_0}{T} \left(ln\frac{T+t}{t} - \frac{T}{t} \right)$$
$$= -\frac{1}{2}\mu_0 \pi abm(h) \cdot \frac{\partial \chi'}{\partial \, ln\omega} \cdot \frac{I_0}{T} \left(ln\frac{T+t}{t} - \frac{T}{t} \right) \tag{9}$$

2.3. Response of Sphere

In this paper only the case of a non-magnetic conducting sphere lying on the axis of the coils will be considered. Following [1], the voltage, normalized by the product $N_t N_r I$, induced in the receiver coil by such a target buried in non-conducting soil ($\sigma_1 = 0$, which makes the equivalent current dipole moment $P_\phi = 0$) can be written as:

$$v^{sphere}(\omega) = i\omega\mu_0 H^b_{1z} M_z \tag{10}$$

where H^b_{1z} is the z component of magnetic field intensity that would be produced in soil at the location of the sphere centre if a unit current were flowing in the receiver coil of radius, b. M_z is the z component of the scatterer equivalent magnetic dipole moment, which for a sphere of radius, R, and electrical parameters, $(\mu_2, \epsilon_2, \sigma_2)$ embedded in a half-space with parameters $(\mu_1, \epsilon_1, \sigma_1)$ can be written as:

$$M_z = -2\pi R^3 H_{1z} \times \frac{[\mu_1(1 + k_2^2 R^2) + 2\mu_2] \, sinh(k_2 R) - (2\mu_2 + \mu_1)k_2 R \, cosh(k_2 R)}{[\mu_1(1 + k_2^2 R^2) - \mu_2] \, sinh(k_2 R) + (\mu_2 - \mu_1)k_2 R \, cosh(k_2 R)} \tag{11}$$

where H_{1z} is the field produced at the sphere centre by unit transmitter current, and $k_2^2 = i\sigma_2\mu_2\omega$. The expression for the in-soil field H_{1z} is given in [1, 2]. The field H^b_{1z} can be also obtained from the same expression by simply replacing a with b and setting $I = 1$.

As in the case of soil, time-domain responses can be calculated by applying inverse Fourier/Laplace transforms to appropriate frequency domain expressions. For example, inverse Laplace transform of $v^{sphere}(s)/s$ would result in the response of the sphere to a step-current excitation. The author is not aware of an analytical solution when the sphere is buried in a soil with general magnetic properties characterized by Equations 1 and 2. In such cases, inverse transforms will be calculated numerically. However, if the sphere is situated in free space, analytical solutions are possible. A detailed theoretical and experimental study of the time domain response of a sphere, which considers both permeable and nonpermeable spheres, higher order induced multipoles (order of spatial mode $n > 1$), the effect of pulse shape and measurement electronics with coils of finite thickness, is given in [15].

[†] An alternate derivation is discussed in [9].

Here only the simpler case which considers a nonpermeable sphere ($\mu_2 = \mu_0$) and only induced dipoles ($n = 1$), and assumes coils to have no thickness will be treated. Following the technique discussed in [15], the step response of the sphere in free space can be written as

$$v_{step}^{sphere}(t) = \frac{3\pi R^3 \mu_0 a^2 b^2}{(h^2 + a^2)^{3/2}(h^2 + b^2)^{3/2}} \cdot \frac{1}{\beta^2} \sum_{m=1}^{\infty} e^{-\frac{m^2 \pi^2}{\beta^2}t} \quad , \text{where} \quad \beta^2 = \mu_0 \sigma_2 R^2 \tag{12}$$

Similarly, one can show that the response to a triangular current pulse of duration T that drops to 0 from its peak value of I_0 at $t = 0$ is given by

$$v_{ramp}^{sphere}(t) = -\frac{I_0}{T} \frac{3\pi R^3 \mu_0 a^2 b^2}{(h^2 + a^2)^{3/2}(h^2 + b^2)^{3/2}}$$

$$\times \left[-\sum_{m=1}^{\infty} \frac{1}{m^2 \pi^2} e^{-\frac{m^2 \pi^2}{\beta^2}(t+T)} U(t+T) + \sum_{m=1}^{\infty} \frac{1}{m^2 \pi^2} e^{-\frac{m^2 \pi^2}{\beta^2}t} U(t) - \frac{T}{\beta^2} \sum_{m=1}^{\infty} e^{-\frac{m^2 \pi^2}{\beta^2}t} U(t) \right] \tag{13}$$

where $t > 0$ and $U(t)$ is a unit step function. Although there would be no occasion to use this particular result in this paper, it is included here for completeness and to indicate that one should be mindful of the pulse shape when analyzing metal detectors. Future work will use this result.

3. DESCRIPTION OF EXPERIMENTS

A report incorporating details of the experimental setup is being prepared. Only a minimal description, sufficient to understand the parameters of the experimental data, is given here. All measurements were conducted using a suitably modified Scheibel AN19/2 metal detector. The sensor coils had the following nominal parameters: (1) transmitter coil - 20 turns with a mean radius of 0.1275m; (2) receiver coil - 33 turns with a mean radius of 0.093m. An external function generator was used to drive the transmitter to produce a unipolar triangular current pulse train with the following parameters: pulse duration, T=132 μs; maximum current, I_0 =3.06 A; and a pulse period of ~150 ms. The receiver amplifier had a d.c. gain of 270 and a 3-dB bandwidth of 200 kHz. The receiver output was sampled every 3 μs and digitized by a 16-bit A/D converter. To obtain improved S/N ratios, 5000 cycles of the output were coherently averaged to arrive at a single response measurement. The transmitter current waveform was simultaneously measured in a similar way. The background response, with the sensor head positioned away from the ground (at a height at least 1.5 m above the ground) and other objects, was periodically measured. The background response was subtracted from the total response in the presence of an object (e.g., soil, metal target) in order to obtain the desired secondary response due only to the object(s). For the data reported in this paper, the target used was an aluminum sphere of radius R = 0.0127 m and conductivity $\sigma_2 = 3.54 \times 10^7$ S/m.

In-air target response was measured in a climate-controlled laboratory of nonmetallic construction. Soil response and in-soil target response were measured using a 2 m deep soil pit with a 4 m×6 m surface, filled with Cambodian laterite. Susceptibility of soil samples was measured using the Bartington MS2B sensor at two frequencies, 465 Hz and 4650 Hz. Six soil samples from the patch of soil over which measurements were made were collected and their susceptibility measured. One of these samples were taken from the spot directly under the center of the coils and the remaining five were all within a transmitter coil radius of this point. The average of the susceptibilities of these samples is assumed to represent an "equivalent" susceptibility for the halfspace model. The accuracy of this assumption will depend on the actual degree of uniformity of the soil and on sensor height. The measured susceptibility values are shown in Table 1.

4. RESULTS

4.1. Soil Response and Estimation of Model Parameters

Measured and theoretical responses of the Cambodian soil are compared in Figure 2 for a number of sensor heights (h). Numerical techniques of transforming frequency-domain results to the time domain, when triangular

Table 1. Measured real part of magnetic susceptibility of soil samples in SI units, a multiplying factor of 10^{-5} being implicit.

Sample No.	Real χ at 465 Hz, χ_{LF}	Real χ at 4650 Hz, χ_{HF}	$\chi_{LF} - \chi_{HF}$
1	252	238	14
2	208	192	16
3	320	306	14
4	249	234	15
5	227	217	10
6	295	279	16
Average	258.5	244.3	14.2

waveforms like the ones used in the experiments are used, are still under development. Partly for that reason, the theoretical responses presented are only the ones calculated using the approximate relation, Equation 9. The slope $\frac{\partial \chi'}{\partial \ln \omega}$ is estimated from the average values of χ_{LF} and χ_{HF} shown in Table 1, and the overall gain of the measurement system is accounted for in calculating the response. Given the approximations involved in deriving Equation 9, experimental uncertainties and inhomogeneity of soil properties, the agreement between measured and calculated responses is considered remarkable. The data also show the rapid decrease of soil signal with sensor height, particularly for times close to current turn-off.

The good agreement seen above means that, when the sought-after response can be cast as a function of $\frac{\partial \chi'}{\partial \ln \omega}$ or χ'' as in Equation 9, one need not explicitly know the values of the individual soil model parameters, namely, χ_0, τ_1 and τ_2. However, in general, knowledge of the values of the individual soil parameters may be needed. For example, the equations used in this paper for calculating fields inside the soil halfspace and the response of a buried target require knowledge of the individual parameters. These equations will be modified in the future to take advantage of the approximate linear (with respect to $\ln \omega$) behaviour of χ in some natural soils, as is done in deriving Equation 9. For now, the general formulation will be used.

The author is not aware of any reliable and accurate method of estimating the individual soil parameters from measurements provided by a readily available instrument. Instruments being developed [13] to measure complex susceptibility of soil over a wide frequency spectrum should allow estimation of individual parameters in the future. In this paper, an ad hoc method is used to get a workable estimate of the parameters through a trial-and-error process. The method followed is described below.

A measured response (the measurement at $h = 0$m was used) is linearly fit to the function represented by Equation 7 to estimate the factor $\frac{\chi_0}{\ln(\tau_2/\tau_1)}$. The fit obtained is very good and the uncertainty in the estimated value of $\frac{\chi_0}{\ln(\tau_2/\tau_1)}$ small. Obviously, knowing an accurate value for this factor does not allow unique determination of the individual parameters. Knowing the general shape of frequency variation of susceptibility, a value of χ_0 is arbitrarily chosen to be one slightly higher than χ_{LF}, in order to restrict the range of possible values of the parameters. This choice fixes the value of $\frac{\tau_2}{\tau_1}$. From this, various pairs of values of τ_2 and τ_1 can be selected for further analysis. The values of χ_0, τ_1 and τ_2 thus selected are then used as initial guesses in a non-linear fitting program that fits Equation 7, treating all three parameters as unknowns, to the same measured data in an attempt to estimate parameter values. With some trial and error a good fit is obtained but, as expected, the uncertainty in parameters are extremely large. The recovered parameters are used in Equation 2 to compute $\chi'(\omega)$, and the calculated values are compared with the two available measured values, namely, χ_{LF} and χ_{HF}. The parameters are then varied in a trial-and-error manner to get a good agreement with the measured slope and values. One set of parameters that produced a reasonable agreement for the average values of χ_{LF} and χ_{HF} in the case of the Cambodian soil are $\chi_0 = 0.003$, $\tau_1 = 10^{-22}$ s and $\tau_2 = 0.5$ s. This set of parameters are simply used, as needed, for the computations in this paper and no claim is made as to their uniqueness or physical significance.

In the future, a better method will be developed to replace the above somewhat ad hoc, crude and cumbersome process. One of the reasons that the non-linear fitting process does not result in more certain parameter estimation is that Equation 7 incorporates the assumption of linearity (with respect to $\ln \omega$) of susceptibility over

the entire frequency spectrum. Equation 7 needs to be replaced by an expression that does not depend on such an approximation of Equation 2. Fitting such a model to measurements may produce better estimates of the individual parameters. Alternatively, if most soils are found from measurements to be linear in behaviour over the frequency band of interest, equations to compute various fields and responses can be modified to obviate the need for individual values of the parameters. All these aspects will be investigated in the future.
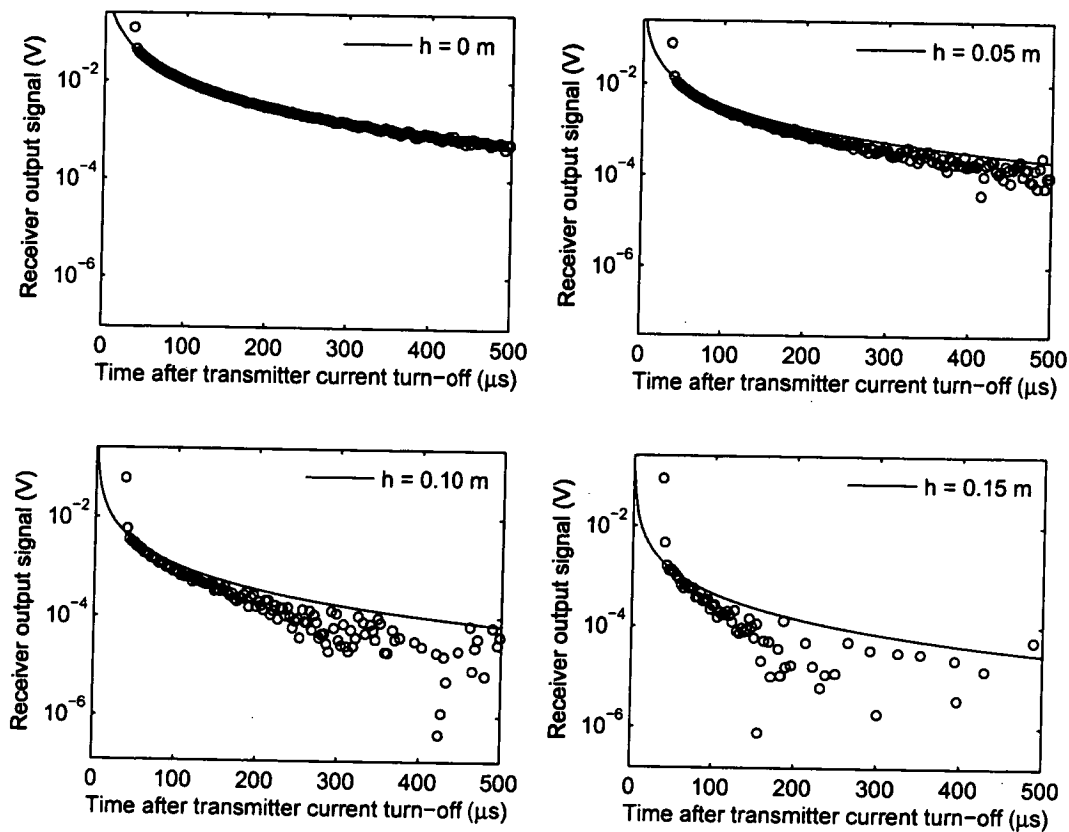
Figure 2. Measured and calculated response of Cambodian soil for a number of sensor heights (h). Solid lines are calculated responses while circles are measured data.

4.2. Conducting Sphere

As mentioned already, numerical techniques of inversion of frequency-domain results to the time domain when triangular waveforms are used are still under development. For this reason, only response due to a step-function excitation, which can be computed using the method in [4], will be used to study the case of a buried sphere. Although practical metal detector systems, including the one used in the experiments here, do not measure such a response, some basic questions regarding the effect of soil can be investigated through the use of the ideal step response. To this end, the response of the aluminum sphere in air and that when it is buried in soil are computed and compared with the response of the soil halfspace alone. As a check on computations, the step response of the sphere in air is computed using two methods: (1) numerical inversion of $v^{sphere}(\omega)/(i\omega)$ from Equation 10; and (2) direct computation using the analytical expression given by Equation 12. Response of the soil is evaluated using numerical inversion of $v^{soil}(\omega)/(i\omega)$ from Equation 4. Figure 3 shows the step response of the aluminum
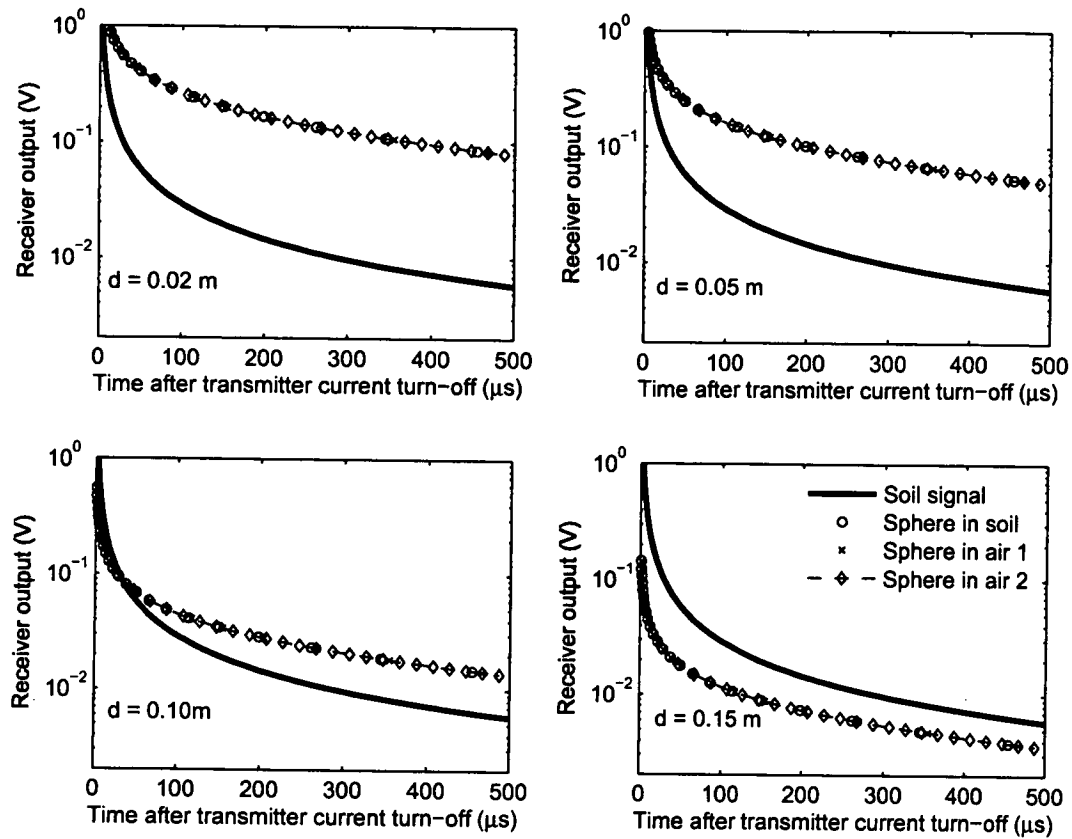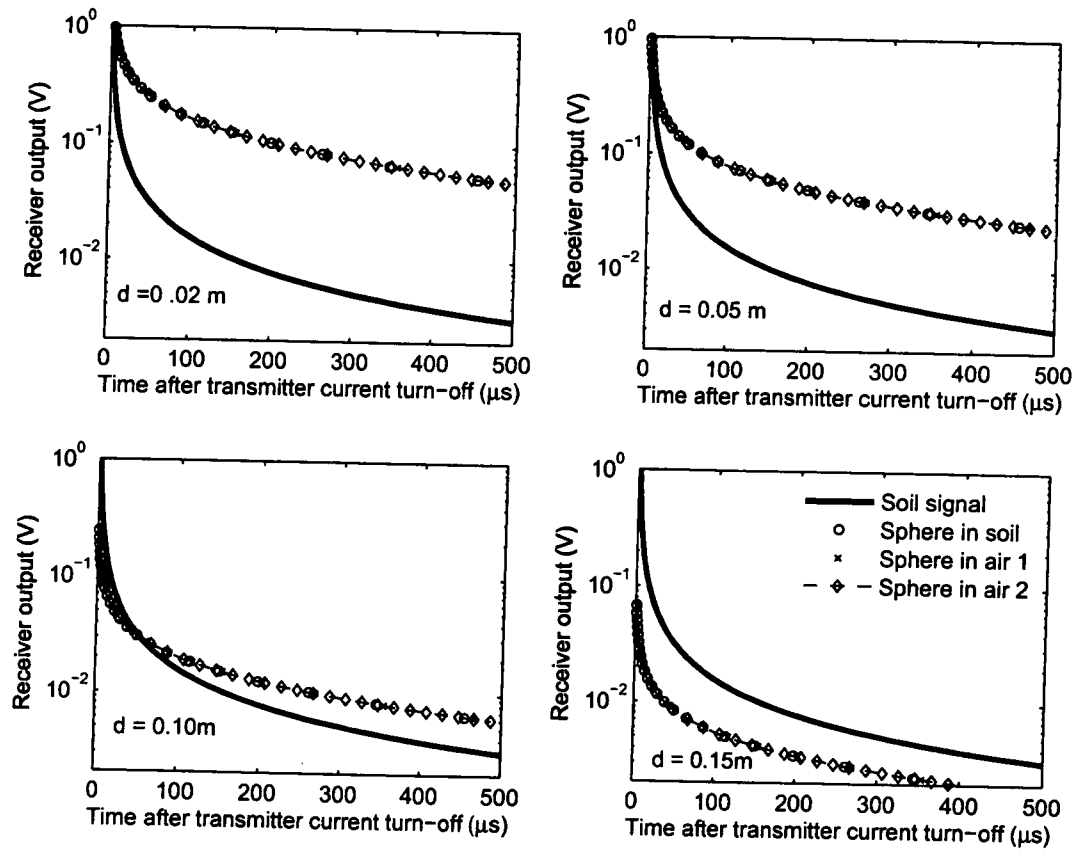
Figure 3. Step response of aluminum sphere in air and in Cambodian lateritic soil for a number of target depths d, compared with the response of the soil for sensor height $h = 0$ m. Response of the sphere in air is computed by two methods: (1) numerical Fourier inversion and (2) evaluation of analytical expression. Soil parameters used are $\chi_0 = 0.003$, $\tau_1 = 10^{-22}$ s and $\tau_2 = 0.5$ s.

sphere in air and in Cambodian lateritic soil for a number of target depths d along with the response of the soil when the sensor is lying on it, that is, $h = 0$ m. For the cases under consideration, an examination of the results shows the following:

(a) Calculation of response of the sphere in air by the two methods produce the same result, which verifies the accuracy of the particular technique of numerical Fourier inversion.

(b) For the soil in question, the response of the sphere in air and in soil are not noticeably different. This would allow the use of the in-air response in the place of in-soil response which could be more difficult to compute in general.

(c) The signal due to the metal sphere dominates the soil signal when the target depth is "shallow", $d < 0.10$ m. But, even for the soil with relatively low susceptibility, the soil signal begins to exceed the signal due to the sphere, which has significant metal content compared with that in some low-metal antipersonnel landmines, when it is buried deeper than about 0.10 m. At a depth as low as 0.10 m, the initial part of the soil signal marginally exceeds the target signal. At $d = 0.15$ m the soil signal completely dominates the target signal.

(d) No definitive statement about the detectability of the target can be made just from the above observations. The output of the detector is the sum of the signal due to the soil and that due to any target. If the soil is spatially uniform one could, in principle, simply balance out the signal due to the soil and detect the target at the same depth as in air. However, in practice the success of such a simple approach will depend on the degree of spatial uniformity of the soil, the degree to which sensor standoff can be maintained a constant, the dynamic range of the receiver system, particular balancing and detection technique employed, and so on. Aside from the question of detection, the relatively strong soil signal could produce false detections if there is small scale spatial variation in soil susceptibility.

(e) The shape of decay of soil signal is different from that of the target signal, a fact that may be exploited for discriminating between the two signals [3].
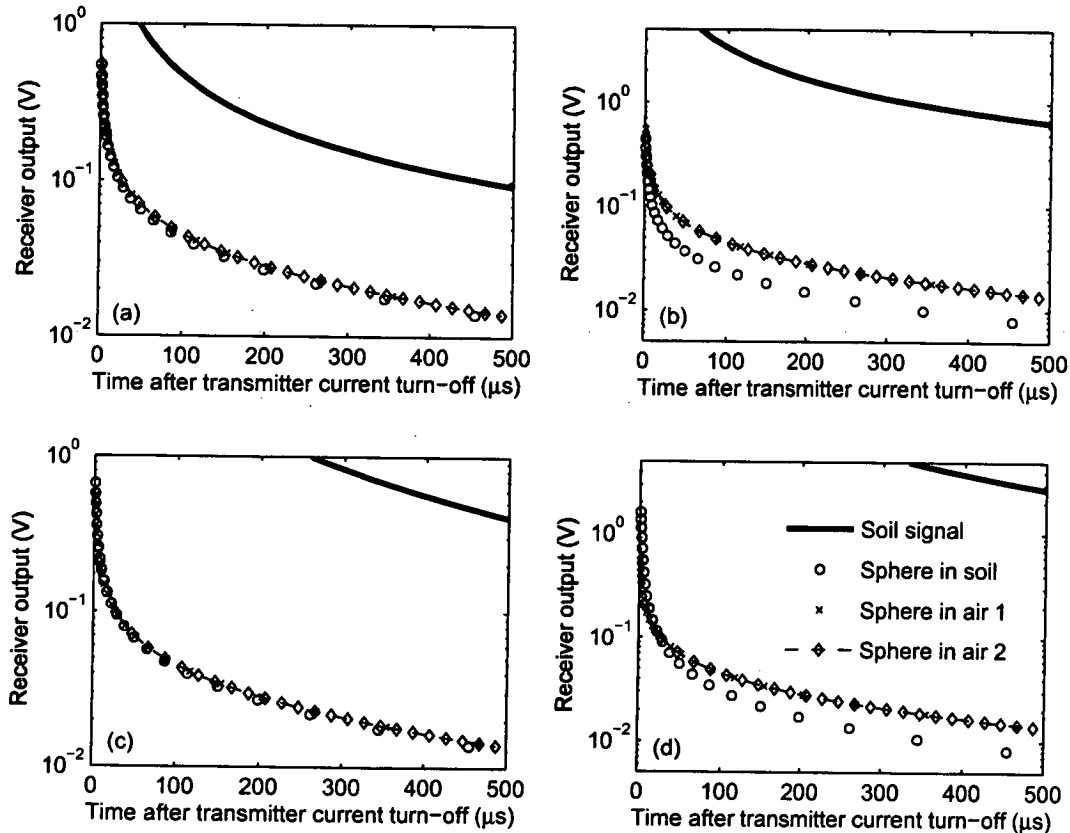

Figure 4. Step response of aluminum sphere in air and in Cambodian lateritic soil for a number of target depths d, compared with the response of the soil for $h = 0.03$ m which is a typical operating sensor height. Other parameters are the same as those for Figure 3.

Figure 4 presents data for the same situations as in Figure 3 expect that the sensor is now used at a more typical operating height of $h = 0.03$ m. Comparison of the two figures show that most of the comments made about Figure 3 also apply to Figure 4. In addition, in Figure 4, the soil signal is reduced due to the increased sensor standoff from the ground surface, which however does not result in a higher ratio of soil to target signal because there is also an accompanying reduction in the target signal due to the increased distance between the

target and the sensor. In fact, for the $d = 0.10$ m case, the initial portion of the soil signal dominates the target signal more when $h = 0.03$ m than when $h = 0$ m. The same comments about detectability as for Figure 3 will apply here as well.

The exact nature of the effect of soil on target signal will depend on the soil parameters which have, so far, been taken as the ones estimated for the particular Cambodian soil used in the experiments. Obviously, it is not possible to present results for all possible values of the parameters χ_0, τ_1 and τ_2. To give an idea of how some other values of these parameters may affect the soil and target signals, the case of the sphere buried at $d = 0.10$ m in soils with four different sets of parameters is shown in Figure 5. The parameters used include some values used in the author's previous work [1, 2] when no measurements of real soils were available. These values are used here for the purposes of continuity and illustration, and no claim is made as to their occurrence in any real-world soil. Figure 5 shows the following:

Figure 5. Step response of aluminum sphere in air and in soils with sets of parameters as follows: (a) $\chi_0 = 0.05, \tau_1 = 10^{-22}$ $s, \tau_2 = 0.5$ s; (b) $\chi_0 = 0.5, \tau_1 = 10^{-22}$ $s, \tau_2 = 0.5$ s; (c) $\chi_0 = 0.05, \tau_1 = 10^{-6}$ $s, \tau_2 = 10^{-3}$ s; (d) $\chi_0 = 0.5, \tau_1 = 10^{-6}$ $s, \tau_2 = 10^{-3}$ s. Sphere depth, d, in all cases is 0.10 m, and sensor height, h, is 0 m.

(i) Because of the much higher values of χ_0 than in the cases considered so far, the soil signal is much higher in general and it exceeds the target signal by a large amount for the depth of burial considered, namely, $d = 0.10$ m. The higher soil signal is expected from Equation 6.

(ii) For the same value of χ_0, the soil signal is higher for the more lossy soil, that is, the one with the lower

value of τ_2/τ_1 (Compare Figure 5 (a) with Figure 5 (c), and Figure 5 (b) with Figure 5 (d)). This behaviour is also expected from Equation 6.

(iii) The effect of the soil on the signal of the sphere is very small (see Figure 5(a) and (c)) even for a value of $\chi_0 = 0.05$, which is more than an order of magnitude higher than that of the Cambodian soil used in the experiments. So, for a lot of natural soils, one may be able to get away with equating the target response in air with that in soil. Although a χ_0 of 0.05 is considered high for natural soils, it is not uncommon. Thus if a detector is able to perfectly cancel out the soil signal (not possible in practice), the detection depth for a target will remain the same as in air.

(iv) For the highest value of χ_0 considered, namely, 0.5, the soil has significant effect on the target signature (see Figure 5(b) and (d)). The values of relaxation time constants involved determine how the time-domain response of the sphere is affected. It is clear that for such a soil, even if the soil signal can be balanced out perfectly, the detection distance in soil would be lower than that in air.

A value of $\chi_0 = 0.5$ is of the order of the highest values found in some "soil lanes" used in landmine detection research (for example, NVESD at Ft. Belvoir have used a lane with $\chi_0 \sim 0.35$).

5. SUMMARY AND DISCUSSION

The electromagnetic induction response of a soil with frequency-dependent magnetic susceptibility and of a small aluminum sphere buried in it were studied in order to understand the adverse effect that some soils occurring in landmine-affected regions can have on metal detectors. Experimental data confirmed numerical prediction that real-world lateritic soil (in this case soil from Cambodia) can produce a strong response which can exceed that due to the buried metal target. Approximate theoretical expressions for very weakly magnetic soils were found to fit the experimental data very well, which allowed the estimation of soil model parameters, albeit in an ad hoc manner.

Although soil signal was found to exceed target signal in many cases, no definitive statement about the detectability of a target in soil can be made just from that observation. The output of the detector is the sum of the signal due to the soil and that due to the target. If the soil is spatially uniform one could, in principle, simply balance out the signal due to the soil and detect the target at the same depth as in air, as long as soil susceptibility is not too high, which is true for a large number of naturally occurring soils. However, in practice the success of such a simple approach will depend on the degree of spatial uniformity of the soil, the degree to which sensor standoff can be maintained a constant, the dynamic range of the receiver system, particular balancing and detection technique employed, and so on. Aside from the question of detection, the relatively strong soil signal could produce false detections if there is small scale spatial variation in soil susceptibility.

Future work will include development of a better method of estimating soil model parameters, investigation of soil and target response using triangular current pulse trains instead of the step current, application of the analysis and experimental verification to more targets and soils, and comparison of results with those obtained by others using different analysis techniques.

REFERENCES

1. Y. Das, "A preliminary investigation of the effects of soil electromagnetic properties on metal detectors," in *Proc. SPIE Conference on Detection and Remediation Technologies for Mines and Mine-like Targets IX*, 5415, pp. 677–690, (Orlando, FL, USA), April 2004.

2. Y. Das, "Electromagnetic induction response of a target buried in conductive and magnetic soil," in *Proc. SPIE Conference on Detection and Remediation Technologies for Mines and Mine-like Targets X*, **5794**, pp. 263–274, (Orlando, FL, USA), March 2005.

3. B. H.Candy, "Pulse induction time domain metal detector." United States Patent Number 5 576 624, November 1996.

4. G. A. Newman, G. W. Hohmann, and W. L. Anderson, "Transient electromagnetic response of a three-dimensional body in a layered earth," *Geophysics* **51**(8), pp. 1608–1627, 1986.

5. S. Chikazumi, *Physics of Magnetism*, Wiley, New York, 1964.

6. G. R. Olhoeft, "Time dependent magnetization and magnetic loss tangents," Master's thesis, Massachusetts Institute of Technology, May 1972.

7. T. Lee, "The effect of a superparamagnetic layer on the transient electromagnetic response of a ground," *Geophysical Prospecting* **32**, pp. 480–496, 1984.

8. L. R. Pasion, S. D. Billings, and D. Oldenburg, "Evaluating the effects of magnetic soils on TEM measurements for UXO detection," in *Proceedings of the UXO/Countermine Forum*, (Orlando, Florida), September 2002.

9. S. D. Billings, L. R. Pasion, D. W. Oldenburg, and J. Foley, "The influence of magnetic viscosity on electromagnetic sensors," in *International Conference on Requirements and Technologies for the Detection, Removal and Neutralization of Landmines and UXO*, H. Sahli, A. M. Bottoms, and J. Cornelis, eds., *Proc. EUDEM2-SCOT - 2003* **1**, pp. 123–130, (Vrije Universiteit Brussel, Brussels, Belgium), September 2003.

10. C. E. Mullins and M. S. Tite, "Magnetic viscosity, quadrature susceptibility, and frequency dependence of susceptibility in single-domain assemblies of magnetite and maghemite," *Journal of Geophysical Research* **78**, pp. 804–809, February 1973.

11. M. Dabas, A. Jolivet, and A. Tabbagh, "Magnetic susceptibility and viscosity of soils in a weak time varying field," *Geophys. J. Int.* **108**, pp. 101–109, 1992.

12. J. Dearing, *Environmental Magnetic Susceptibility: Using the Bartington MS2 System*, Chi Publishing, 35 Birches Lane, Kenilworth CV8 2AB, England, 1994.

13. G. F. West and R. C. Bailey, "An instrument for measuring complex magnetic susceptibility of soils," in *Proc. SPIE Conference on Detection and Remediation Technologies for Mines and Mine-like Targets X*, **5794**, pp. 124–134, (Orlando, FL, USA), March 2005.

14. Y. L. Luke, *Integrals of Bessel Functions*, McGraw-Hill Book Company, Inc., New York, 1962.

15. Y. Das, J. McFee, and R. Chesney, "Time domain response of a sphere in the field of a coil:theory and experiment," *IEEE Transactions on GeoScience and Remote Sensing* **GE-22**(4), pp. 360–367, 1984.